Available online at www.sciencedirect.com
SCIENCE DIRECT®
ELSEVIER
Bioorganic & Medicinal Chemistry 12 (2004) 1315–1324
Bioorganic & Medicinal Chemistry

# Electrochemical release from gold–thiolate electrodes for controlled insertion of ion channels into bilayer membranes

M. B. Buchmann, T. M. Fyles* and T. Sutherland

*Department of Chemistry, University of Victoria, Victoria, BC, Canada V8W 3P6*

Received 12 December 2002; revised 11 June 2003; accepted 12 June 2003

**Abstract**—A proof-of-principle experiment to inject a sub-attomole amount of a channel compound into a bilayer membrane is described. The system is based on reductive cleavage of a self-assembled gold–thiol monolayer. In 'macroscopic' experiments, 11-biphenyloxyundecane thiol formed well-ordered monolayers by open-circuit or controlled potential deposition. The products of reductive release were determined by chromatographic analysis. In DMF, the sole reduction product is the corresponding disulfide. In acetonitrile and water, only the thiol is detected. The current efficiency is low due to competing electrolysis of water, and to the low solubility of the released thiol or disulfide layer. On a 'microscopic' scale, the half ester of dithiodibutyric acid with gramicidin was deposited on a gold microelectrode under open circuit conditions. The thoroughly washed microelectrode, placed in proximity to a bilayer, released gramicidin only following a 100 ms pulse of reducing potential. The transfer efficiency of this method for controlled positioning of ion channels is estimated to be better than 1 part in $10^5$.


## 1. Introduction

The field of synthetic ion channels has witnessed an explosion during the past decade. As recently as 1996, one of us co-authored a review, fully confident that it was comprehensive up to the submission date.[1] The present Symposium-in-Print amply illustrates that 'comprehensive' coverage of the current field is probably impossible and certain to be passed by events of the next few years, if not months. Collectively, our achievements of the past decade are remarkable: a host of different and unique structural motifs give rise to rapid, selective, and controlled ion transport through bilayer membranes (reviews[2–4]). If a transporter is seen as a 'catalyst of translocation' then the specific conductance and lifetimes now commonly reported (30 pS; 500 ms; 100 mV) equate to catalytic rates ($10^8$ $s^{-1}$) and turnover numbers ($2\times10^8$) that rival (and surpass) natural ion channels. The same cannot be said for parallel developments in the field of synthetic enzymatic catalysis.[5]

Even as we justly celebrate our successes in reproducing *functions* of natural channels, it is obvious that we have a much poorer understanding of the active *structures* of many of the compounds we have reported. Like many areas of supramolecular chemistry, groups with a strong synthetic focus have dominated the early stages, and this has produced a huge of array of structural types. Within a given type, transport function can be controlled through structural variations, yet very dissimilar structural types can produce very similar transport functions. To cite only one example: the specific conductance and ion selectivity parameters of our *bis*-macrocyclic bolaamphiphiles are very similar to the same parameters of the cholate-derived channels reported by Kobuke.[6] These types of coincidences imply that the role of the transporter is to stabilize a partly aqueous environment for ion transfer. Many membrane-spanning structures can achieve this, with the result that many structures will produce similar functional outcomes.

This mechanistic hypothesis has a number of implications for new technologies based on ion channels. From a synthetic perspective, it places more emphasis on the efficiency and flexibility of the synthetic sequence that produces the structures. Many reported ion channels, our own included, are forever doomed as laboratory curiosities since they only arise through lengthy and inefficient syntheses. Much of our recent effort has directly confronted this issue. In our own case, the inefficiencies initially arose through the use of symmetrical

*Keywords:* Gold–thiol self-assembled monolayer; Reduction; Bilayer; Gramicidin.
* Corresponding author. Tel.: +1-250-721-7150; fax: +1-250-721-7147; e-mail: tmf@uvic.ca

0968-0896/$ - see front matter © 2003 Elsevier Ltd. All rights reserved.
doi:10.1016/j.bmc.2003.06.004

bi-functional macrocyclic building blocks. Following a poor-yielding macrocyclization step, a sequence of symmetry-lowering steps, also low yielding, eventually produced the desired compounds with their remarkable transport functions.[7–10] We have recently shown, in two different bis-macrocycle systems, that the macrocycles are unnecessary for transport function, and can be simply replaced by related acyclic units.[11–13] The net result is that many months of synthetic toil can be replaced by a few weeks effort leading to equally functional final products. Linear and branched bolaamphiphiles show the way to a solid-phase synthesis that will allow a diversity of structures to be even more rapidly prepared from a pool of acyclic building blocks.[14]

With recent progress on synthesis, comes the realization that there are other critical-path issues surrounding the integration of synthetic ion channels into new technologies. Our own focus is on a system that will reproduce the features of electrical signaling along axons.[15,16] There are numerous design criteria for the channels required (selectivity, rectification, self-inhibition) that will require considerable synthetic effort and structure–activity optimization. In addition to these chemical parameters, are a number of physical parameters. In nature, the ion channels in myelinated nerves are located at the 'nodes of Ranvier' spaced along the length of the axon cell.[16] More generally, the localization and orientation of all natural channels is under precise cellular control. In contrast the common methods for incorporation of synthetic channels into bilayers are both haphazard and profoundly wasteful. In a typical bilayer clamp experiment an amount of compound is injected into solution adjacent to a patch of membrane. 'Small' molecules can be injected as a solution in methanol or DMSO; larger molecules are often injected using a carrier vesicle (liposome) that subsequently fuses with the planar bilayer. In either case the amount of compound is 'small'—typically 10–100 nanomoles—but the experiment actually observes only a few tens of molecules. This represents incorporation efficiency no better than 1 part in $10^{14}$! Pre-mixing of channel and lipid components before formation of the planar bilayer has the required mass-transfer efficiency, but this method foregoes the possibility of directional insertion to produce a defined orientation of the channel in the bilayer. Such orientation is essential for voltage-gating[9,17,18] and other vectorial membrane phenomena.

If we are to approach ionic signal propagation in an artificial system, we must have controlled insertion of a defined amount of compound into a defined patch of membrane with preservation of orientation. This means a short diffusion step through the aqueous phase to allow the hydrophobic-hydrophilic balance in the released compound to produce the self-assembled active structure with the correct orientation in the membrane. Consequently we are interested in ways to produce a pulse of a few thousand molecules at a defined point within a few microns of the membrane surface. Our conceptual design is illustrated in Figure 1. We envisage a gold microelectrode on a micromanipulator placed in proximity to the bilayer. The active transporter would

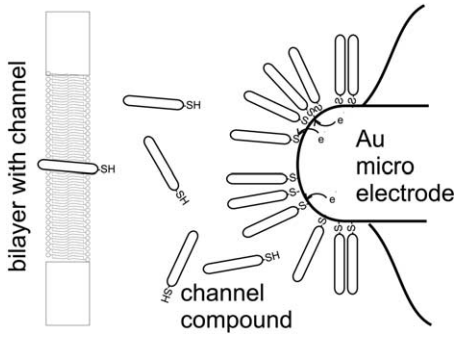


**Figure 1.** Sketch of the proposed release system (not to scale).

be immobilized on the surface of the electrode via a gold–thiol interaction. At the time of release, the Au–S bond would be reductively cleaved, releasing the transporter into solution. Diffusion from this high local concentration should be fast and some fraction of the released material should insert and produce the required oriented and functional ion channel.

Reductive release from gold–thiol self-assembled monolayers (Au–S SAMs) has been studied electrochemically.[19–23] There is now good agreement that the initial electrochemical step is a one-electron reduction that occurs at about −1.2 V versus. SCE. The monolayer packing, the electrolyte, and the gold crystal face all influence the reduction potential, so for polycrystalline gold a range of potentials is common. The released thiolate can reabsorb once the electrode potential shifts below a reduction threshold, and there is evidence that poorly soluble thiols/thiolates remain with the electrode after release.[20] Apart from reports of a 'thiol odor', the nature of the products has not been investigated. With respect to the proposal of Figure 1 there a number of unknowns: What species is (are) released into bulk solution (thiol, thiolate, disulfide)? What type of control is available (electrode area, reduction time)? What are the quantitative aspects (current efficiency, does released material simply reattach)? In related work on reductive cleavage of thiobuytrate esters, we have shown that the release step could potentially be made irreversible through intramolecular thiolysis of the ester.[24] This 'traceless linker approach' would have the advantage that the ion channel would not need to be a thiol.

Our goals in the current study are to focus on the principal unknowns as listed above. We examine the electrochemistry of an Au–SAM in a 'macroscopic' system in order to detect, identify, and quantify the products of reductive cleavage. We then turn to a 'microscopic' experiment in which a gramicidin derivative is released in a proof-of-concept experiment as sketched in Figure 1. Some quantitative detail will distinguish the 'macroscopic' and 'microscopic' experiments. A well-ordered SAM from an alkyl thiol on single-crystal Au(111) has $10^{14}$ molecules per $cm^2$.[25] The macroscopic experiment uses an electrode area of 1.5 $cm^2$ in contact with an electrolyte volume of 1.0 mL. Full release to the bulk solution is expected to give solution concentrations in the range of 10–100 nM. Provided a suitable fluorophore is present in the release product(s), this level is

appropriate for analysis by HPLC with fluorescence detection. The microscopic experiment uses a gold microelectrode with a tip area of $3\times10^{-5}$ cm$^2$. This would release a maximum of $10^8$ molecules from a well-ordered monolayer for detection via insertion in a bilayer. The nominal 'bulk' concentration in this 'microscopic' experiment is less than 100 attomolar, nine orders of magnitude lower than in the 'macroscopic' experiment.

## 2. Results and discussion

### 2.1. 'Macroscopic' reductive release

The thiol for this experiment is required to form well-ordered SAMs and allow for quantitative detection at nanomolar levels. In addition to the Au–S interaction, the stability and ordering of SAMs is related to efficient alkyl chain packing, so the required thiols should also contain an extended polymethylene segment. These requirements are met in the biphenyl-thiol **3**, the synthesis of which is given in Scheme 1.

The synthesis proceeds directly from commercially available 4-biphenol and 11-bromoundecanol via alkylation of the phenoxide to produce the ether **1**. The primary alcohol of **1** was converted to the bromide **2** and then, via basic hydrolysis of the corresponding thiouronium salt to the thiol **3**. Depending on the oxygen exposure, a mixture of thiol **3** and disulfide **4** could be produced. Pure disulfide is produced by titration with iodine. From pure **4**, the pure thiol **3** is readily produced by zinc-acid reduction. Both **3** and **4** show limited solubility in many solvents, although millimolar solutions can be prepared in THF, methanol, ethanol, DMF, and acetonitrile. As expected, excitation at the UV absorption maximum (265 nm) produces a strong fluorescence centered at 330 nm. Isocratic liquid chromatography on C-18 reversed phase with acetonitrile as eluent allows separation of **3** and **4**, and quantification by fluorescence detection. The detector response for both compounds is linear over six orders of magnitude with a detection limit (3 times the standard deviation of a blank intercept) of 0.9 nM for **3** based on a 20 μL sample injection. Thus **3** and **4** fulfill the analytical requirements for determination of the reductive release product(s) on the 'macroscopic' scale.

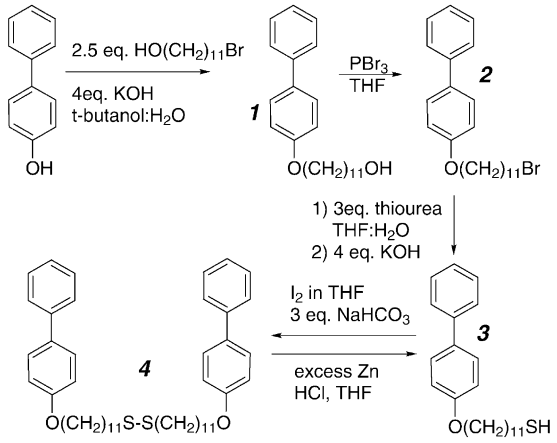


**Scheme 1.** Synthesis of the fluorescent thiol and disulfide for macroscopic release experiments.

The quantitative determination of release at the expected levels requires a cell that can be cleaned to trace levels yet possesses a large, and highly reproducible, electrode area in contact with a limited electrolyte volume. Our solution to this problem was a Teflon cell in the shape of a small beaker with the base formed from Au-coated glass slides. These slides are clamped to form a smooth, leak-free contact with the cell wall. The inside diameter of the cell then defines the electrode area. The glass slide is replaced for each experiment, and the separate cell components can be extensively cleaned. The cell permits an electrolyte volume of 1.0 mL to contact an electrode area of 1.5 cm$^2$. The Au slide is the working electrode, a Ag/AgCl wire linked by an agar bridge acts as the reference, and the counter electrode is an Au or Pt wire. Cathodic and anodic processes thus occur in the same solution, but the experiments are of short duration to minimize secondary reaction products. All the electrochemistry used a custom built potentiostat designed to give highly reproducible and rapid response.[26]

Monolayer formation under open-circuit conditions was simply achieved by immersion of the Au electrode in millimolar ethanolic solutions of **3** or **4** overnight, followed by extensive solvent and water rinsing. SAMs can also be formed from **3** by the controlled-potential method reported by Lennox,[27] in which the working electrode is held at +0.6 V (versus Ag/AgCl) for 15 min with nitrogen bubble agitation. The second method is certainly faster, and produces superior SAMs. Monolayer integrity was assessed by the conventional method of cyclic voltametry of a ferri/ferrocyanide probe ion in a contacting electrolyte (Fig. 2A).[28,29] A bare electrode shows the expected redox wave, and the peak current is progressively decreased as the number of defects in the SAM decreases. Although this method shows that high-quality monolayers are formed correctly, it introduces additional trace contaminants into the system, and these interfered with the subsequent analysis.

Determination of monolayer integrity without contaminant introduction was achieved by measuring the time response of the current following a transient shift in potential. The response time of the charging of the electrode interface is a sensitive function of the monolayer coverage, as illustrated in Figure 2B. At a bare electrode, the response time is relatively slow, as diffusive events are required to establish a double-layer. At a SAM-coated electrode, the double layer charging is minor, and the capacitor is restricted to the insulating monolayer itself, hence does not involve diffusion. Figure 2B also shows the result of a partial reductive cleavage from a SAM electrode: the opening of defects in the monolayer is clearly detected by this method.

Although neither of the techniques used to determine monolayer integrity are quantitative measures of the

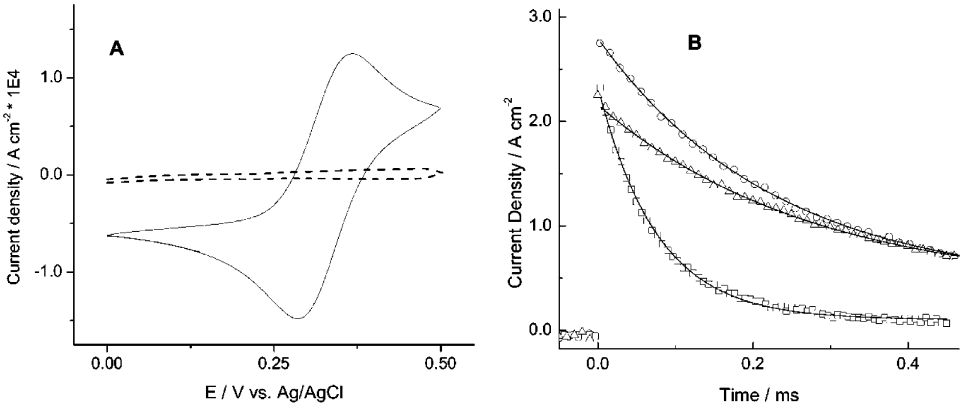


**Figure 2.** Methods for characterization of SAMs: (A): cyclic voltamograms of a bare Au surface (solid line) and a SAM coated Au surface (dashed line) [10 mM $K_3Fe(CN)_6$, 1 M KCl, 100 mV $s^{-1}$ versus Ag/AgCl]; (B): capacitive charging of a bare Au surface (circles), a SAM-coated Au surface (squares), a partly reduced SAM (triangle) (1 M $LiClO_4$, potential versus Ag/AgCl switched from −0.1 to 0.0 V at $t = 0$).

numbers of defect sites present, both are quite sensitive to the presence of small numbers of defects.[30] Over a series of experiments that varied the deposition conditions (time, solvent, temperature), it was possible to define 'standard' conditions for the reproducible formation of well-ordered, low-defect SAMs. Thus analysis of every SAM produced was not essential— and thus did not introduce any contaminants! Reproducibility between independent replicates treated this way was ±10%.

The reductive release in the 'macroscopic' system was studied in water, acetonitrile, and DMF using $LiClO_4$ and $Bu_4NPF_6$ as supporting electrolyte. In all experiments, a cleaned Au–SAM was mounted in the cell, a known volume of elecrolyte was added and subjected to a square-wave shift to −2.0 V (versus Ag/AgCl) for a controlled duration (typically a few milliseconds). An aliquot of the electrolyte solution was then immediately (within a minute) removed for subsequent analysis by liquid chromatography. The cell was then cleaned, and the process repeated for some different reductive duration. The results in DMF are illustrated in Figure 3.

Two types of measurements are to be compared: determination of the number of electrons delivered to the electrode and determination of the identity and amount of the product(s) formed. Figure 3A gives a typical chronoamperometric response for one sample. The trace shows capacitive charging and discharging at the ends of the 5 ms pulse of reducing potential and the current can be integrated over the duration of the pulse to give the amount of charge passed. Figure 3B shows the results for several such experiments with reductive periods of up to 100 ms. No plateau is reached, and the amount of current passed greatly exceeds the expected amount required to cleave the SAM. The additional current is due to anodic processes, probably water oxidation, and thus chronoamperometry does not provide a direct way to observe the release.

The results of the chromatographic analysis are given in Figure 3C. The sole detected product in this experiment in DMF is the disulfide **4**. This unexpected result is general for all experiments done in DMF. It is unlikely that the disulfide arise simply by oxidation by either trace oxygen or at the anode. Experiments in other solvents show the formation of only **3**, so the experimental procedure is capable of detecting the thiol had it formed and escaped to the bulk solution. The amount of **4** released is quantified by integration of the peak centered at 15.7 min, and the results are given in Figure 3-D. Unlike the coulometric experiment, the amount released does rapidly achieve a plateau. Nearly all the material eventually detected in bulk solution is released within a 5-ms reduction period. However, the total released is significantly less than expected. As above, the number of molecules is taken to be $10^{14}$ $cm^{-2}$, a value derived for single crystal Au. The surface roughness factor of gold sputtered on glass is reported to be 2.0[31] giving a total of $3\times10^{14}$ molecules as the maximum expected in the experiment. The plateau value in Figure 3-D lies at about 20% of this value.

Table 1 summarizes this experiment in three different solvents. Note that the thiol **3** is the sole detected product in water or acetonitrile. Only DMF gives the disulfide **4** as the released species. The amount of **3** released to bulk aqueous solution is very low and does not build up even at very long reduction times (5 s). This likely represents the concentration of a saturated solution. Even short reductive periods are sufficient to open up defects in the monolayer as assessed by the techniques discussed, so it is likely that the Au–S interaction is cleaved rather quickly, but the released material is non-specifically associated with the electrode and not available for dissolution in the bulk solvent. The acetonitrile result is perhaps an intermediate case between water, where **3** is very insoluble, and DMF, where both **3** and **4** are appreciably soluble. Even so, there is clearly non-specific adsorption of material even in acetonitrile that is visible on the recovered electrode as a birefringent coating in reflected light. This cannot be **3** alone, and must involve some solvent and electrolyte in order to develop a sufficient thickness to interact with visible light. Reduction occurs quickly with respect to diffusional processes, hence the local concentration is very high. If a diffusion rate of $10^{-5}$ cm $s^{-1}$ is assumed, the concentration within 1 μm of the electrode exceeds 0.1 M for at least a second following the reductive pulse.

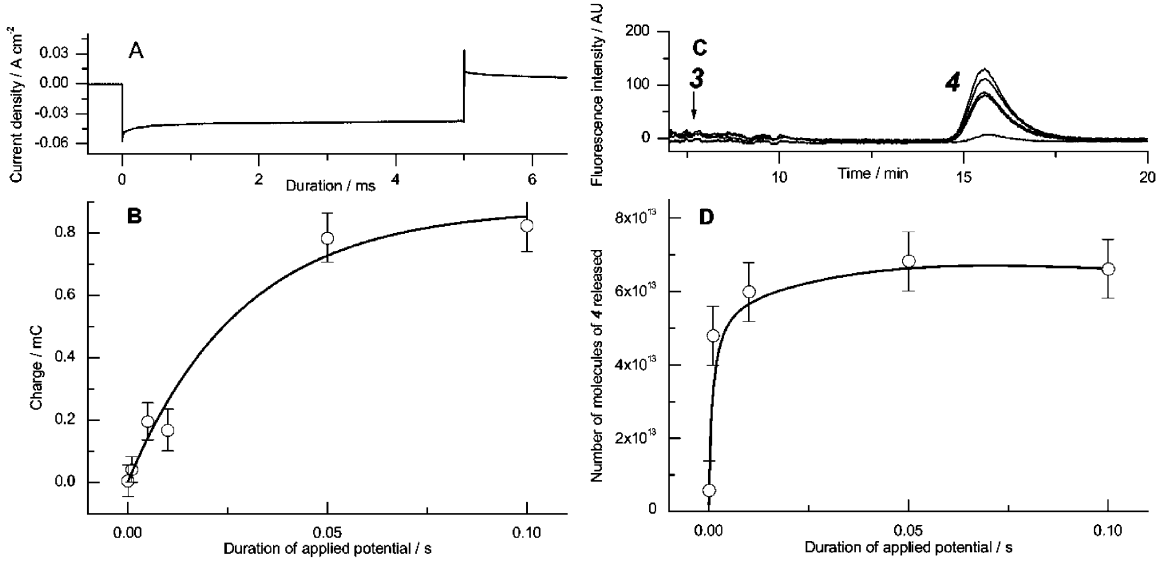


**Figure 3.** Reductive release from **3**-coated SAM in DMF (1 M $LiClO_4$): (A): chronoamperometric trace (−2.0 V versus Ag/AgCl, 5 ms duration); (B): Charge as a function of the duration of the reducing potential (integration of A for the pulse duration); (C): HPLC trace of samples from different reduction durations (C-18, MeCN eluent, 40 °C, fluorescence detection excited at 265 nm, detected at 330 nm); (D): concentration of released **4** as function of the reduction duration (integrated area of peaks in C).

**Table 1.** Summary of data on 'macroscopic' reductive release[a]

| | DMF | MeCN | $H_2O$ |
|---|---|---|---|
| Duration (ms)[b] | 10 | 500 | 500 |
| Charge passed (mC) | 0.17 | 2.8 | 8.7 |
| Detected species[c] | **4** | **3** | **3** |
| Conc. ($M\times10^8$) | 6.6 | 4.0 | 0.12 |
| Electrons/molecule | 18 | 450 | 54,000 |

[a] $LiClO_4$ electrolyte; results similar with $Bu_4NPF_6$ electrolyte in DMF and MeCN.
[b] Duration of the reduction potential to give the charge and concentration parameters for the rows below.
[c] Sole species detected in all cases.

Quite apart from events near the cathode, the very poor current efficiencies signal that oxidative processes are significant in all three solvents. The applied potential exceeds the water-splitting potential in both water and acetonitrile, so the current efficiencies are not surprising.

The results from the 'macroscopic' experiments allow a number of conclusions of relevance to the goal of controlled release. The first is that thiol/thiolate is the expected product in water. A reductive pulse of a few milliseconds duration will be sufficient to break all the Au–S interactions at the surface and produce a 'plug' of thiol/thiolate in the immediate vicinity of the electrode. Dependent upon the solubility of the released species, the amount that will be released to bulk solution for diffusion to the membrane will be smaller than the total amount released, due to precipitation and adsorption. The majority of channel-forming compounds are quite hydrophobic, so this loss will be a significant factor. At the same time, the competing water splitting process will be dominant in any real application for release. Taken together, these two factors effectively limit any quantitative control over the release through control of reduction pulse duration. In a practical reductive release, the quantitative control must arise via control of the amount of material present, both through the size of the electrode, and through the packing density of the compound of interest on the electrode. The smallest available microelectrodes have a surface capacity that vastly exceeds the few molecules required for a transport experiment, so this is not a serious limitation.

## 2.2. 'Microscopic' reductive release

We turn now to a proof of principle experiment in which the bilayer clamp will be used as the detector for an even smaller amount of material released. We require an active channel-forming compound that is well characterized through conventional methods of introduction. The compound also requires a thiol or disulfide linkage to allow immobilization on the electrode. We chose to modify gramicidin with the thiobutyrate linkage we have previously investigated as a 'traceless' linker. The synthesis and reaction of this compound **6** are given in Scheme 2.

One equivalent of dithiodibutyric acid (**5**) was activated with di-isopropylcarbodimide (DIC) in the presence of the acylation catalyst DMAP (dimethylaminopyridine) and then coupled with one equivalent of thoroughly dried gramicidin. Exploratory work had established that the diester was not formed, so the half-ester **6** was the desired target. The peptidic products were freed of small-molecule reaction biproducts by size exclusion chromatography. The isolated material gave additional $^{13}C$ NMR signals consistent with the formation of **6** and the MALDI-MS showed peaks consistent with a sodium adduct of **6**, together with sodium adduct ions for underivatized gramicidin. A daughter-ion scan established that these latter ions are not fragments of **6** but arise as impurities. Analysis by HPLC confirmed the presence of free gramicidin together with a peak assigned to **6**. We were unable to find suitable chromatographic conditions to isolate **6** free of all unreacted gramicidin. Since only **6** would be covalently linked to

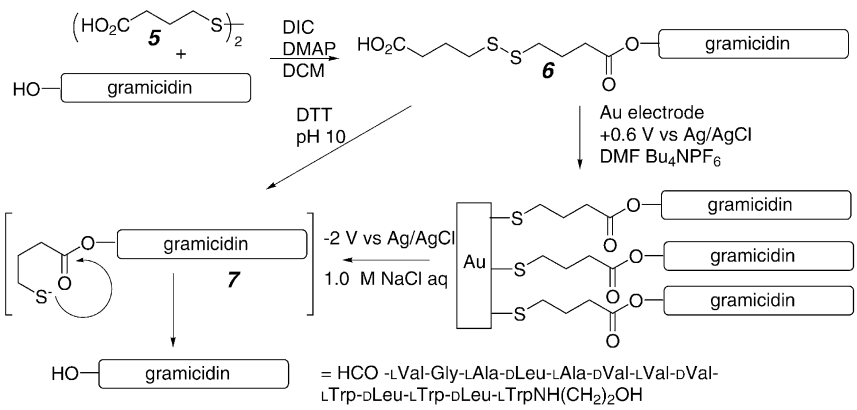


**Scheme 2.** Synthesis and reactions of the half-ester of dithiodibuyric acid (**5**) with gramicidin.

the Au electrode, the impurity gramicidin can potentially be removed by washing after linkage to the Au electrode. The purity of the sample used in subsequent experiments was >90% **6** with <10% gramicidin based on LC analysis assuming equal molar absorptivity in the UV spectra of **6** and gramicidin.

We were concerned that this thiobutyrate ester derivative might not react quickly enough to release native gramicidin via the intermediate thiolate (or thiol) **7** (Scheme 2). Accordingly we treated a sample of **6** with dithiothreitol (DTT), and followed the reaction through analysis of samples by LSIMS, MALDI-MS and HPLC. Samples were submitted to these techniques immediately following their treatment with DTT/NaOD. MALDI-MS clearly showed complete conversion of the thiobutyrate ester to native gramicidin after 1 h of sample and instrument preparation. HPLC analysis confirmed the complete conversion within a 5-min period before sample dilution and analysis. The DTT reduction is rapid only under basic conditions where ester hydrolysis also occurs at a slower rate.[24] The newly released thiolate at the gold electrode would experience a local pH that is basic immediately following release, similar to the conditions of these experiments.

We were also concerned to investigate the channel-forming potential of **6**. The mixed sample of predominantly **6** with impurity gramicidin readily forms channels following injection of a methanolic solution to a typical bilayer clamp experiment. The specific conductance determined for the mixture was the same as for native gramicidin under the same conditions (18.6 pS; 1 M NaCl pH 4). There are two possibilities: **6** is completely inactive, and we observe only the residual gramicidin in this experiment, or the channels formed by **6** and gramicidin are indistinguishable under these conditions. Other gramicidin derivatives modified as **6** at the reduced C-terminal position produce channels,[32,33] so it is likely that the channels formed by **6** are sufficiently similar to those from native gramicidin as to be indistinguishable by conductance measurements.

Finally, the experiment envisaged by Figure 1 was done using a 60-μm diameter Au wire as a microelectrode. Open-circuit deposition of **6** on the electrode tip was followed by a thorough washing sequence including a period of sonication in ethanol. We are quite confident that native gramicidin would have been removed from any surface under these washing conditions. The electrode was mounted on a micromanipulator and positioned within 50 μm of a bilayer formed in a bilayer clamp cell as assessed visually (binocular microscope) through a comparison of the electrode diameter and the distance to the bilayer. With the electrode held in close proximity, the bilayer clamp experiment recorded a 30-min period of data with the membrane held at a potential of 100 mV. The results are given in Figure 4A. Apart from a few irregular spikes, there is no activity evident. The microelectrode was then subjected to a single square-wave pulse of −2 V versus Ag/AgCl of 100 ms duration. As soon as the bilayer clamp recording could be started, the activity shown in Figure 4B was recorded. Due to electrical inteferences between the potentiostat and the bilayer clamp, the two experiments were 'independent' in the sense that while one was active the other was disconnected. There is a time delay between the two halves of Figure 4, of about a minute to accomplish the electrical connections–disconnections required.

The activity following release is clearly due to gramicidin that has been introduced in the system by the reductive pulse. The system settles to a single channel record as shown in the late part of Figure 4B, which has

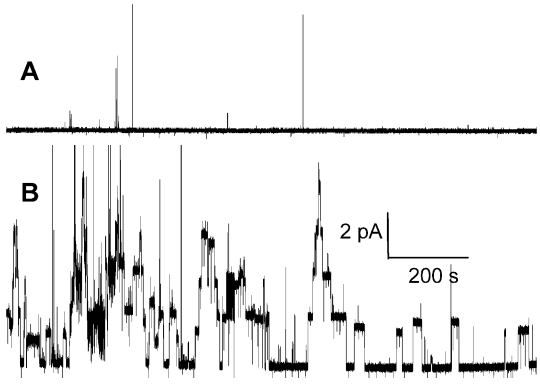


**Figure 4.** Bilayer conductance (di-phytanoyl PC, 1 M KCl, +100 mV) before (**A**) and after (**B**) release of gramicidin by reduction of an Au-SAM of **6** (−2.0 V versus Ag/AgCl, 100 ms). There is less than a 1-min delay between the end of **A** and the beginning of **B**.

the expected specific conductance of 18 pS. As noted above, we cannot say if this is native gramicidin, **6**, or some hybrid channel of the two. The recording also shows up to four sets of gramicidin dimer channels active simultaneously. Thus at least eight molecules have been injected. Given that the frequency of opening declines within this record, as expected for a dilution of gramicidin within the bilayer volume, it is likely that there are more than eight molecules involved. It would be reasonable to assume that of the order of $10^2$ molecules have been introduced to the bilayer. The area of the starting electrode is sufficiently large to accommodate of the order of $10^8$ molecules assuming a tightly packed monolayer of $10^{14}$ molecules $cm^{-2}$. It is very unlikely that the layer formed by **6** can achieve this packing density: a close packed array of gramicidin estimated from a plane perpendicular to the long axis of the gramicidin dimer in crystal structures[34,35] has packing density 10-fold lower. Even this packing density is unlikely as the thiol attachment to the surface would inhibit the formation of tightly packed dimers as found in the crystal lattice, and the short contact time for adsorption would inhibit the formation of well-ordered structures. Fewer than $10^7$ molecules on the microelectrode is probably a realistic estimate. Thus the incorporation efficiency (molecules observed/molecules introduced to the system) can be estimated to be better than 1 part in $10^5$. This represents at least seven orders of magnitude improvement over haphazard incorporation from injection of solutions of gramicidin to the bilayer clamp system under comparable conditions.

## 3. Conclusions

So what? What has this study achieved? On the most general level, the products of reductive release from Au-thiolate SAMs have been directly detected and quantified. Much less material than expected is released due to poor current efficiency and non-specific adsorption of released material on the electrode. But some amount is released—the disulfide in DMF solution, thiol/thiolate in aqueous solution—and the bond cleavage part of the process is rapid. Thus the 'macroscopic' experiments establish that a pulse of material can be injected from an Au-SAM electrode. This result is similar to a recent report of electrochemical release of NO under conditions on the scale of our 'macroscopic' experiment.[36] Together with the use of a thiobutyrate linkage, electrochemical release is extended to include species that are not themselves the products of electrochemical reaction, and to the very much smaller amounts involved in our 'microscopic' conditions. Of course, the release need not be limited to channel-forming compounds. The amounts available from conventional microelectrodes would be compatible with single-cell level injection of other proteins, DNA, or small bioactive molecules.

The physical control over channel positioning is an essential component in many potential applications of synthetic ion channels. The nanotechnology revealed in nature relies on such positional control, and we infer that it will prove to have a functional significance. In our own application, the present demonstration allows us to plan the next stages, so that at some future date the chemical and physical components of a signaling system akin to an axon can be assembled to work in concert.

## 4. Experimental

### 4.1. Synthesis

**4.1.1. 11-(1,1′-Biphenyl-4-yloxy)-1-undecanol (1).** To a suspension of KOH (9.0 g, 160 mmol, 4 equiv) in 25:3 (*tert*-butyl alcohol:$H_2O$) (250 mL), 11-bromo undecan-1-ol (10.0 g, 40 mmol) and biphenyl-4-ol (17.02 g, 100 mmol, 2.5 equiv) were added and the mixture was stirred at reflux for 3 h. The crude cooled slurry was filtered and the residue was dissolved in $CHCl_3$ which was then washed with water (3×50 mL), dried over $Na_2SO_4$, and the solvent was removed under reduced pressure to yield **1** as a white solid (9.25 g, 68%.) $^1$H NMR 300 MHz ($CDCl_3$): δ 7.54 (m, 4H), 7.40 (t, $J$ = 7.4 Hz, 2H), 7.28 (t, $J$ = 7.4 Hz, 1H), 6.95 (m, 2H), 3.98 (t, $J$ = 5.9 Hz, 2H), 3.62 (t, $J$ = 6.6 Hz, 2H), 1.79 (qn, $J$ = 7.4 Hz, 2H), 1.4 (m, 17H). $^{13}$C NMR 75.47 MHz ($CDCl_3$): δ 158.7, 140.9, 133.5, 128.7, 128.1, 126.7, 126.6, 114.8, 68.1, 63.1, 32.8, 29.6, 29.6, 29.5, 29.4, 29.4, 29.3, 26.1, 25.7. EI exact mass: calculated for $C_{23}H_{32}O_2$: 340.2402, found: 340.2402.

**4.1.2. 1,1′-Biphenyl-4-yl 11-bromoundecyl ether (2).** To a solution of **1** (9.25 g, 27 mmol) in THF (50 mL), $PBr_3$ (5.2g, 3-fold excess) was slowly added over 10 min at 50 °C. Following 50 min at reflux, the solution was brought to room temperature where water was added to quench excess $PBr_3$. The solution was extracted with $CH_2Cl_2$ (3×20 mL) and the combined organic extracts were dried over $Na_2SO_4$. Removal of solvent under reduced pressure produced a yellow solid that was triturated to purity with warm pentane to yield **2** as a white solid (2.95 g, 27%). $^1$H NMR 300 MHz ($CDCl_3$): σ 7.53 (m, 4H), 7.40 (m, 2H), 7.29 (m, 1H), 6.96 (m, 2H), 3.99 (t, $J$ = 6.6 Hz, 2H), 3.40 (t, $J$ = 6.6 Hz, 2H), 1.82 (m, 4H), 1.4 (m, 14H). EI exact mass: calculated for $C_{23}H_{31}BrO$: 402.1558, found: 402.1555.

**4.1.3. 11-(1,1′-Biphenyl-4-yloxy)-1-undecanethiol (3).** The bromide **2** (2.95 g, 7.3 mmol) was combined with thiourea (3 equiv) in a 9:1 mixture of THF/$H_2O$ (100 mL) and stirred at reflux for 48 h. The mixture was cooled and KOH (1.8 g) was added and the reflux continued for another 8 h. The mixture was cooled then acidified with 1.0 M HCl to pH 2, then extracted with $CH_2Cl_2$ (3×20 mL). The combined organic extracts were dried over $Na_2SO_4$ and the solvent was removed under reduced pressure to give **3** as a white solid (2.36 g, 90%). Mp 65–66 °C. $^1$H NMR 300 MHz ($CDCl_3$) δ 7.55 (m, 4H), 7.42 (m, 2H), 7.32 (m, 1H) 6.96 (m, 2H), 4.00 (t, $J$ = 6.6 Hz, 2H), 2.51 (q, $J$ = 7.4 Hz, 2H), 1.80 (qn, $J$ = 6.6 Hz, 2H), 1.60 (qn, $J$ = 7.4 Hz, 2H) 1.3–1.55 (m, 15H). $^{13}$C NMR 75 MHz ($CDCl_3$): δ 158.8, 141.0, 133.6, 128.8, 128.2, 126.8, 126.7, 114.9, 68.2, 34.2, 29.7, 29.6,

29.5, 29.4, 29.2, 28.5, 26.2, 24.8. EI exact mass: calculated for $C_{23}H_{32}OS$: 356.2174, found: 356.2177. Some preparations afforded the thiol contaminated with some disulfide **4**. Pure **3** could be obtained from **4** by reduction: **4** (1 equiv) was dissolved in THF (7 mL for 100 mg of compound) and Zn (10 equiv) and HCl (30 equiv) was added. The mixture was refluxed for 16 h, cooled, then extracted with $CH_2Cl_2$ (3×10 mL). The combined organic extracts were washed with 10 mL of 10% $NaHCO_3$ then $H_2O$ (2×10 mL), dried over $Na_2SO_4$ then the solvent was removed under reduced pressure producing a white solid. The solid was dissolved in a minimum amount of hot 95% EtOH and slowly cooled. The solid product was filtered and rinsed with cold EtOH to yield pure **3** as a white powder.

**4.1.4. Bis(11-(1,1′-biphenyl-4-yloxy)undecyl) disulfide (4).** A saturated solution of $I_2$ (3 g) in THF (10 mL) was added dropwise to the thiol (110 mg, 0.31 mmol) dissolved in THF (5 mL) at 50 °C containing $NaHCO_3$ (80 mg), until a yellow color persisted for 30 min. The solvent was removed under reduced pressure, $H_2O$ (10 mL) was added and the solution was extracted with $CH_2Cl_2$ (3×10 mL). The combined organic extracts were dried over $Na_2SO_4$, and the solvent was removed under reduced pressure producing a yellow solid. The crude product was dissolved in a minimum amount of hot 100% EtOH that was then slowly brought to room temperature to yield a white precipitate. The solid was filtered and washed with cold 100% EtOH to give **4** on drying (80 mg, 40%). Mp 109–111 °C. $^1$H NMR 300 MHz ($CDCl_3$): δ 7.55 (m, 4H), 7.42 (m, 2H), 7.32 (m, 1H) 6.96 (m, 2H), 3.98 (t, $J$ = 5.9 Hz, 2H), 2.67 (t, $J$ = 7.4 Hz, 2H), 1.79 (qn, $J$ = 8.1 Hz, 2H), 1.66 (qn, $J$ = 7.4 Hz, 2H) 1.3–1.60 (m, 15H). $^{13}$C NMR 75 MHz ($CDCl_3$): δ 158.8, 141.0, 133.6, 128.8, 128.2, 126.8, 126.7, 114.9, 68.2, 39.4, 29.7, 29.7, 29.6, 29.5, 29.5, 29.4, 28.7, 26.2. EI exact mass: calculated for $C_{46}H_{62}O_2S_2$: 710.4191, found: 710.4198.

**4.1.5. Gramicidin monoester of 4-4-dithiodibutanoic acid (6).** Diisopropylcarbodiimide (DIC; 150 mg, 1.19 mmol) was dissolved in distilled dichloromethane (30 mL) follwed by 4-dimethylaminopyridine (DMAP; 8 mg, 0.06 mmol) and 4,4-dithiodibutyric acid (143 mg, 0.601 mmol). This mixture was stirred for 7 min and dried gramicidin (1.08 g, 0.574 mmol) was added. (The gramicidin was dried under high vacuum for 5 h prior to use.) The reaction mixture was stirred at 40 °C for 24 h. The entire reaction mixture was then placed on a LH-20 size exclusion column and a mixture of gramicidin and **6** was eluted with 4:3 $CHCl_3$ and MeOH. On removal of solvent this procedure yielded 637 mg of white crystalline powder that was found to be >90% **6** and the remainder unreacted gramicidin. $^{13}$C NMR (DMSO-$d_6$): 169.3,62.4, 56.3, 54.9, 45.0 in addition to peaks for gramicidin. MALDI-TOF MS (monoisotopic mass, intensity, formula, calculated mass): 1904.32, 100%, $C_{99}H_{140}N_{20}O_{17}Na$, 1904.06 (gramicidin + Na); 2169.26, 53%, $C_{107}H_{151}N_{20}O_{20}S_2Na_3$, (**6** Na salt + Na); 2169.06; 1918.33, 14%, $C_{99}H_{138}N_{20}O_{18}$, 1918.04 (gramicidin isoform + Na); 2183.38, $C_{107}H_{149}N_{20}O_{21}S_2Na_3$ (isoform of **6** Na salt + Na); 2165.45, 48%, (2183 ion − $H_2O$). HPLC (C18 reverse phase, 80% MeOH/20% water/0.1% TFA adjusted to pH 3.0 with triethylamine, 1.0 mL/min, 5 uL of 0.1 M phenol internal standard eluted at 2.960–2.975 min, detection by UV at 254 nm): 10.9 min (gramicidin, 5%), 28.5 min (**6**, 95%). A 0.0667 M dithiothreitol (DTT) solution was prepared by the addition of DTT (28.1 mg, 0.182 mmol) to 2.73 mL of 0.1 M NaOH (0.272 mmol). An aliquot of this DTT solution (45 μL, 3.0 μmol) was added to 6 (5.3 mg, approx. 2.5 μmol) in 500 uL of MeOH. Analysis of the product mixture by MALDI-TOF MS within 1 h: 1881 (24%, gramicidin + H), 1904 (100%, gramicidin + Na), 1918 (16%, gramicidin isoform + Na), no other peaks above 1925 $m/z$. Analysis of a separate product mixture prepared in the same fashion followed by HPLC within 5 min: 7.3 min (15%, gramicidin isoform), 10.6 min (85%, gramicidin), no peaks after 15 min.

### 4.2. 'Macroscopic' reductive release

All aqueous solutions were made from Nano-pure™ water with a resistivity of 18 MΩ cm. Concentrated $H_2SO_4$, $H_2O_2$, KCl, AgCl, $KNO_3$, $CH_2Cl_2$, EtOH, tetrabutylammonium hexaflorophosphate, and $K_3Fe(CN)_6$, were used as supplied. Acetonitrile (MeCN) was distilled over 4 Å molecular sieves, DMF was distilled from a $CaH_2$ slurry and stored over 4 Å molecular sieves and $LiClO_4$ was three times recrystallized from $H_2O$ before use. Gold-coated glass slides were purchased from EMF, Albany NY, USA. Gold surfaces were cleaned in freshly prepared piranha solution (70% $H_2SO_4$/9% $H_2O_2$) by submersion for 30 min with periodic agitation to free surface bound bubbles. *Caution: piranha solution is a powerful oxidizer, can react violently with organic materials and should be stored in containers that prevent pressure build up*. After extensive rinsing (5×10 mL of water followed by 5×10 mL of EtOH) the gold was dried with a stream of nitrogen.

### 4.3. Electrochemical instrumentation

The instrumentation consists of three components: a potentiostat, a function generator and a data acquisition device. The function generator was purchased from Gage-Applied Instruments and the data acquisition was done through a digital oscilloscope purchased from Pico Technology Limited, UK interfaced through a PC running PicoScope software. The potentiostat was a custom-built instrument optimized for measuring fast current jumps.[26]

A schematic diagram of the electrochemical cell is given as Figure 5. The securing posts (copper screws) exert clamping pressure on the Teflon housing to ensure a leak-free contact with the Au surface. An O-ring was also placed under the Au-glass slide to compensate for surface deformities in the underlying Teflon that could potentially crack the glass under pressure. The geometric exposed surface area was 1.5 $cm^2$ in a cell volume of 1.0 mL. Electrical connection to the Au-glass slide was made by a small, flat-nosed alligator clip, and was verified to be <1 Ω resistance before each experiment.

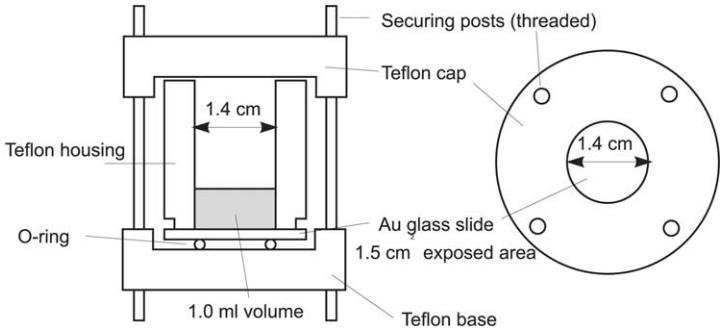


**Figure 5.** Top and side views of the electrochemical cell.

### 4.4. Monolayer formation by open-circuit incubation

The thiol or disulfide was dissolved in ethanol to a concentration of 1 mM. The gold surface was then allowed to sit in the thiol solution at room temperature with periodic, stirring for 24 h to establish a monolayer. After 24 h, the gold was removed, rinsed ($5\times10$ mL $CH_2Cl_2$ then $5\times10$ mL EtOH and finally $5\times10$ mL $H_2O$) and dried under a stream of nitrogen. Surfaces can be stored in a cool dark place under an inert atmosphere for a period of up to 1 week.

### 4.5. Monolayer formation by potential-assisted deposition[27]

A 1 mM thiol solution in MeCN containing 1 M $LiClO_4$ or 1 M tetra-butylammonium hexaflorophosphate electrolyte was placed in a conventional three-electrode electrochemical cell. The working electrode was the gold-glass slide, the counter-electrode was a platinum mesh and the reference electrode was an Ag/AgCl wire in 1 M KCl. The reference solution made ionic contact with the deposition solution via a 1% agar filled U-tube containing 2 M $KNO_3$. A potential of $+0.6$ V versus Ag/AgCl was applied for 15 min while the solution was stirred by a stream of bubbles of nitrogen gas. The resulting monolayer was rinsed in the same manner as the above incubation method. Additionally, it was found that storage in water for 24 h immediately after monolayer formation yields a more insulating monolayer.

### 4.6. Monolayer characterization by cyclic voltametry

The gold surface is placed into a conventional three-electrode electrochemical cell (Pt mesh counter electrode, Ag/AgCl in 3 M KCl reference and gold working electrode) containing 1 M KCl and 10 mM $K_3Fe(CN)_6$. Cyclic voltametry was performed by a PAR 273A potentiostat controlled by CorrWare™ software (Scribner and Associates). The input triangle waveform had vertex positions at 0.0 and 0.5 V versus the reference. Typically, five cycles were run at a rate of 100 mV $s^{-1}$ where only the last cycle was recorded. Data files were plotted using CorrView™ software (Scribner and Associates). Monolayer coverage was established by taking the ratio of $i_{peak}$ of oxidation ($+0.3$ V versus Ag/AgCl) of bare gold to $i_{peak}$ of oxidation of monolayer-covered gold. Typically, values were 80 or greater.

### 4.7. Monolayer characterization by capacitance measurements

All measurements were recorded in a grounded Faraday cage; the computer monitor was also encased in a Faraday cage to directly eliminate most noise from this source. The monolayer coated gold surface was placed in its custom Teflon housing and electrical contact was made by a small alligator clip. The counter electrode was a gold wire (area of 0.2 $cm^2$) and the reference electrode was Ag/AgCl linked via the agar bridge (above) with 1 M $LiClO_4$ as electrolyte. The experiment uses a 100 mV potential step (1-s duration) from $-0.1$ to 0.0 V. The curve fits were done to an equivalent circuit of a resistor (R1) and capacitor (C1) in parallel followed by a second resistor in series (R2 where $R2 \ll R1$). Thus: $i(t) = (E0/R1)\times\exp(-t/\tau)$ where E0 is the potential step and $\tau = R1C1\times R2$ The $i(t)$ data were fit using Origin 6.1.

### 4.8. Washing

During the course of the trace analysis, it became apparent that extensive washings between experiments was essential. Eventually this extended to the point where all the components involved in the release experiment were disposable except the Teflon housing and counter electrode. The Teflon housing and counter electrode were rinsed in 10 volumes of $CH_2Cl_2$ and then boiled in Nano-pure™ $H_2O$ for 2 h with two water changes then placed in a heated sonication bath of 100% ethanol for 10 min. This extensive washing procedure was necessary because of the poor solubility of **3** and **4** and their particular affinity for glass.

### 4.9. Analysis of 3 and 4 by liquid chromatography

Separation was accomplished with an RP-C18 column (250 mm×2 mm ID, Macherey-Nagel). Samples (20 μL injection loop) were eluted with 100% $CH_3CN$ with 0.1% trifluoroacetic acid added. At 50 °C under the above solvent conditions, **3** eluted at 4.0 min and **4** at 11.0 min. At 40 °C **3** eluted at 7.7 min and **4** at 15.7 min. The eluent was monitored by fluorescence using the $\lambda_{max}$ of **3** (265 nm) as the excitation wavelength and monitoring its emission peak (330 nm). The calibration of fluorescence intensity with concentration was linear over six orders of magnitude with a limit of detection of 0.9 nM for **3**; **4** is about twice as easily detected.

### 4.10. 'Microscopic' reductive release

Our procedures for the bilayer clamp experiment have been recently reported and were used here without alteration (diphytanoyl phosphatidyl choline; 1.0 M NaCl pH 4 citrate buffer electrolyte).[12] The Au microelectrode (wire from 100 mesh Au gauze, 63 μm diameter; Alfa-Aesar) was cleaned and **6** was deposited under open circuit conditions from a 1-mM solution in ethanol. The electrode tip was allowed to touch the solution surface for 10 s. The monolayer coated electrode was then immediately rinsed (5×10 mL $CH_2Cl_2$ then 5×10 mL EtOH and finally 5×10 mL $H_2O$) and dried under a stream of nitrogen. The electrochemical release and the bilayer clamp were done independently of one another, that is as one experiment was underway the other was in the off state with all power sources disconnected and all electrical connections placed within the Faraday cage to limit antennae effects. The Au microelectrode was fastened to the manipulator arm an X-Y-Z manipulator on a grounded microscope stage and connected to the potentiostat via a BNC cable. The positioning of the electrode required the bilayer clamp to be 'off' because of electrical noise from the light source. Once a bilayer was established the microelectrode was positioned close (within a distance equivalent to one electrode diameter estimated visually) to the aperture in the trans compartment. A 0.17 $cm^2$ Au wire counter electrode was placed next to it. The Ag/AgCl electrode in the trans compartment used in the bilayer clamp experiment doubled as a reference electrode. Once the microelectrode was positioned, 30 min of bilayer conductance data under +100 mV clamp conditions were recorded. The reductive cleavage was then done (−2 V; 1 s) with the bilayer clamp in the standby mode. Immediately following the cleavage recording under +100 mV clamp conditions continued.

## Acknowledgements

The ongoing support of the Natural Sciences and Engineering Research Council of Canada is gratefully acknowledged.

## References and notes

1. Fyles, T. M.; van Straaten-Nijenhuis, W. F. In *Comprehensive Supramolecular Chemistry*; Reinhoudt, D. N., Ed.; Elsevier Science: Amsterdam/New York, 1996; Vol. 10, p 53.
2. Matile, S. *Chem. Soc. Rev.* **2001**, *30*, 158.
3. Gokel, G. W.; Mukhopadhyay, A. *Chem. Soc. Rev.* **2001**, *30*, 274.
4. Kobuke Y. In *Advances in Supramolecular Chemistry*; Gokel, G. W., Ed.; JAI: Greenwich, CT, 1997; Vol. 4, p 163.
5. Sanders, J. K. M. *Chem. Eur. J.* **1998**, *4*, 1378.
6. Yoshino, N.; Satake, A.; Kobuke, Y. *Angew Chem. Int. Ed. Eng.* **2001**, *40*, 457.
7. Cross, G. G.; Fyles, T. M.; James, T. D.; Zojaji, M. *Synlett* **1993**, 449.
8. Fyles, T. M.; Loock, D.; van Straaten-Nijenhuis, W. F.; Zhou, X. *J. Org. Chem.* **1996**, *61*, 8866.
9. Fyles, T. M.; Loock, D.; Zhou, X. *J. Am. Chem. Soc.* **1998**, *120*, 2997.
10. Cameron, L. M.; Fyles, T. M.; Hu, C. J. *Org Chem.* **2002**, *67*, 1548.
11. Fyles, T. M.; Hu, C.; Knoy, R. *Org. Lett.* **2001**, *3*, 1335.
12. Eggers, P. K.; Fyles, T. M.; Mitchell, K. D. D.; Sutherland, T. *J. Org. Chem.* **2003**, *68*, 1050.
13. Fyles, T. M.; Hu, C. *J. Supramol. Chem.* **2001**, *1*, 207.
14. Hu C. PhD Thesis, University of Victoria; Victoria, 2002.
15. Hille, B. *Ionic Channels of Excitable Membranes*, 2nd ed; Sinauer Associates, Incorporated: Sunderland, 1992.
16. Sargent, P. B. In *An Introduction to Molecular Neurobiology*; Hall, Z. W., Ed.; Sinauer Assoc: Sunderland, MA, 1992; pp 33–80.
17. Goto, C.; Yamamura, M.; Satake, A.; Kobuke, Y. *J. Am Chem Soc.* **2001**, *123*, 12152.
18. Kobuke, Y.; Ueda, K.; Sokabe, M. *Chem. Lett.* **1995**, 435.
19. Yang, D. F.; Morin, M. *J. Electroanal Chem.* **1997**, *429*, 1.
20. Yang, D. F.; Wilde, C. P.; Morin, M. *Langmuir* **1997**, *13*, 243.
21. Kawaguchi, T.; Yasuda, H.; Shimazu, K.; Porter, M. D. *Langmuir* **2000**, *16*, 9830.
22. Walczak, M. M.; Popenoe, D. D.; Deinhammer, R. S.; Lamp, B. D.; Chung, C. K.; Porter, M. D. *Langmuir* **1991**, *7*, 2687.
23. Imabayashi, S.; Iida, M.; Hobara, D.; Feng, Z. Q.; Niki, K.; Kakiuchi, T. *J. Electroanal Chem.* **1997**, *428*, 33.
24. Buchmann, M. B.; Fyles, T. M.; Mischki, T.; Sutherland, T.; Tong, C. C.; Yip, V. L. Y. *Arkivoc* **2001**, *2* (U9).
25. Dubois, L. H.; Nuzzo, R. G. *Ann. Rev. Phys. Chem.* **1992**, *43*, 437.
26. Labayen M. PhD Thesis, University of Victoria; Victoria, BC, 2002.
27. Ma, F. Y.; Lennox, R. B. *Langmuir* **2000**, *16*, 6188.
28. Bandyopadhyay, K.; Patil, V.; Sastry, M.; Vijayamohanan, K. *Langmuir* **1998**, *14*, 3808.
29. Bandyopadhyay, K.; Vijayamohanan, K. *Langmuir* **1998**, *14*, 625.
30. Takehara, K.; Takemura, H.; Ide, Y. *Electrochim. Acta* **1994**, *39*, 817.
31. Schlenoff, J. B.; Li, M.; Ly, H. *J. Am. Chem. Soc.* **1995**, *117*, 12528.
32. Woolley, G. A.; Jaikaran, A. S. I.; Zhang, Z. H.; Peng, S. Y. *J. Am Chem Soc.* **1995**, *117*, 4448.
33. Woolley, G. A.; Zunic, V.; Karanicolas, J.; Jaikaran, A. S. I.; Starostin, A. V. *Biophys. J.* **1997**, *73*, 2465.
34. Wallace, B. A.; Ravikumar, K. *Science* **1988**, *241*, 181.
35. Langs, D. A. *Science* **1988**, *241*, 188.
36. Hou, Y.; Chem, Y.; Amro, N. A.; Wadu-Mesthrige, K.; Andreana, P. R.; Liu, G.; Wang, P. G. *Chem. Commun.* **2000**, 1831.